Collinear dissipative weakly coupled acousto-optical states governed by the acoustic waves of finite amplitude in a two-mode medium with linear optical losses

Alexandre S. Shcherbakov,[1,3] Adan Omar Arellanes,[1,*] and Sergey A. Nemov[2,4]

[1]*National Institute for Astrophysics, Optics & Electronics (INAOE), Puebla 72000, Mexico*
[2]*Saint—Petersburg State Polytechnic University, Polytechnicheskaya Str. 29, St-Petersburg 195251, Russia*
[3]*e-mail: alex@inaoep.mx*
[4]*e-mail: nemov_s@mail.ru*
**Corresponding author: arellaneso@inaoep.mx*

Received December 9, 2013; revised March 18, 2014; accepted March 18, 2014;
posted March 25, 2014 (Doc. ID 202305); published April 16, 2014

The components of dissipative weakly coupled states, originating due to collinear Bragg light scattering by the acoustic wave of finite amplitude, are investigated in the square-law nonlinear medium with the linear optical losses. A novel theoretical model is developed for three-wave weakly coupled states of various pulse profiles, propagating in the quasi-stationary regime with the phase mismatch. The availability of both compact and infinite support is analyzed and compared with one another. Two limiting cases for cnoidal profiles are considered in detail and estimated. Their optical components are observed during the acousto-optical experiments in an α-quartz crystalline cell with calibrated optical losses.

OCIS codes: (190.4975) Parametric processes; (250.5530) Pulse propagation and temporal solitons; (190.4223) Nonlinear wave mixing; (350.5500) Propagation.
http://dx.doi.org/10.1364/JOSAB.31.000953

1. INTRODUCTION

The light scattering in a two-mode optically transparent medium modulated by a relatively slow nonoptical wave demonstrates an example of the parametric process in a system with square-law nonlinearity [1,2]. This phenomenon allows for originating a family of multiwave solitary states and solitons, whose field components can be physically distinct from one another, but these components are parametrically coupled [3]. The investigations of acousto-optical interaction using waves of finite amplitude in liquids have been carried out at first in the late 1950s [4,5]. While in solids, these studies have their roots in the 1970s within experimental verification of the Brillouin diffraction theory at very high acoustic frequencies in lead molybdate [6]. Asymmetric light scattering by ultrasonic pulses has been also studied [7]. Further, efforts have been made to describe the light diffraction by ultrasonic pulses using both analytical and numerical methods [8]. Later, the studies of collinear acoustic-optic interaction have shown the dependence of the transmission function on the amplitude of acoustic wave in a specific continuous-wave [9] and pulsed regimes [10]. Even up to now, the acousto-optic interaction occurred by ultrasonic waves of finite amplitude in liquids is under investigation [11]. Together with this, multiwave coupled states in lossless two-mode media had been studied [12,13]. The next step in our investigations had been done within theoretical analysis and experiments related to dissipative solitary waves [14], namely, to collinear three-wave coupled states in a medium with nonoptical losses [15]. Now, in contrast to all the previous considerations, a new specific regime with lossless slow nonoptical wave, but with optical losses is extracted for consideration. In so doing, the Bragg light scattering by acoustic waves of finite amplitude in a two-mode medium exhibiting linear optical losses is elucidated. We develop a new quasi-stationary analytical model describing the localized coupled states with various pulse profiles that include what is essential: the phase mismatches. Attention is paid to cnoidal profiles of the localized weakly coupled states. In particular, two limiting cases for cnoidal profiles associated with infinite support (i.e., hyperbolic secant function) as well as with compact support (i.e., rectangular one) of acoustic wave are considered in detail, numerically estimated, and characterized graphically. In practice, the presence of the linear optical losses in a medium affects identifying the optical components in the experiments with weakly coupled acousto-optical states. Finally, we present the exploited experimental setup and the data obtained due to proof-of-principle experiments directed to observing the optical components of dissipative three-wave weakly coupled acousto-optical states with the phase mismatch in the specially designed collinear AOC made of the x-ray irradiated α-quartz crystal providing the given optical losses.

2. THREE-WAVE INTERACTION WITH THE PHASE MISMATCHES AND LINEAR OPTICAL LOSSES

Let us start from a three-wave codirectional collinear interaction with the mismatched wave numbers in a two-mode

medium, which is described by a set of three nonlinear partial differential equations [12]. Here, we consider the regime of so-called weak coupling [15], when two light modes are scattered by a relatively slow acoustic wave of finite amplitude, exhibiting practically negligible linear losses, when essentially effective Bragg scattering of light can be achieved without any observable influence of the scattering process on that acoustic wave. Then the velocities of light modes can be approximated by the same value c because usually the length of crystalline materials does not exceed 20 cm. In this regime, the above-mentioned set of equations falls into an equation for the complex amplitude $u(x,t)$ of a slow acoustic wave (V is the group velocity of this wave) and a pair of the combined equations for the complex amplitudes $a_0(x,t)$ and $a_1(x,t)$ of the incident (pumping) and scattered light waves, respectively:

$$\frac{\partial u}{\partial x}+\frac{1}{V}\frac{\partial u}{\partial t}\approx 0, \tag{1a}$$

$$\frac{\partial a_0}{\partial x}+\alpha_0 a_0+\frac{1}{c}\frac{\partial a_0}{\partial t}=-q_1 a_1 u\ \exp(2i\eta x), \tag{1b}$$

$$\frac{\partial a_1}{\partial x}+\alpha_1 a_1+\frac{1}{c}\frac{\partial a_1}{\partial t}=q_0 a_0 u^*\ \exp(-2i\eta x), \tag{1c}$$

where $q_{0,1}$ are the constants of interaction, 2η is the mismatch of wave numbers inherent in the interacting waves, and the factors $\alpha_{0,1}$ describe the linear losses of optical waves. One can put $\alpha_0\approx\alpha_1\approx\alpha$ because the frequency shift between optical modes equals to the acoustic frequency ($\sim 10^8$ Hz), which is much smaller than the optical frequencies ($\sim 10^{15}$ Hz). The general solution to Eq. (1a) with the boundary condition $u(x=0,t)=U(t)$ has the form $U[t-(x/V)]$. The reduction of Eqs. (1b) and (1c) is physically motivated by obvious incommensurability between the group velocities of acoustic and two optical waves. One can estimate the summands in the left-hand sides supposing that the interaction takes place only in a limited space area X occupied by an acoustic pulse. The first summands can be estimated by the ratio $\partial a_{0,1}/\partial x\approx A/X$; the second summands describe the optical losses representing rather slow process, so that $\alpha a_{0,1}<A/X$, where A is some amplitude. The third summands lead to $c^{-1}\cdot\partial a_{0,1}/\partial x\approx (V/c)(A/X)$, which means that these terms are the smallest ones in these expressions, and they can be omitted. Thus Eqs. (1b) and (1c) can be reduced down to

$$\frac{\partial a_0}{\partial x}+\alpha a_0=-q_1 a_1 U[t-(x/V)]\exp(2i\eta x), \tag{2a}$$

$$\frac{\partial a_1}{\partial x}+\alpha a_1=q_0 a_0 U^*[t-(x/V)]\exp(-2i\eta x). \tag{2b}$$

Equations (2) include the dependence on time and allow the following relation $J^2(x)=J_0^2\exp(-2\alpha x)$, where $J_0^2=J^2(x=0)$ and $J^2(x)=q_0|a_0|^2+q_1|a_1|^2$. At this step, one can use the substitution $a_{0,1}=f_{0,1}(x,t)\cdot\exp(-\alpha x)$ to convert Eq. (2) to

$$\frac{\partial^2 f_0}{\partial x^2}-\left[2i\eta+\left(\frac{1}{U}\right)\left(\frac{\partial U}{\partial x}\right)\right]\frac{\partial f_0}{\partial x}+q_0 q_1|U|^2 f_0=0, \tag{3a}$$

$$\frac{\partial^2 f_1}{\partial x^2}-\left[-2i\eta+\left(\frac{1}{U^*}\right)\left(\frac{\partial U^*}{\partial x}\right)\right]\frac{\partial f_1}{\partial x}+q_0 q_1|U|^2 f_1=0 \tag{3b}$$

with $q_0|f_0|^2+q_1|f_1|^2=q_0 J_0^2-\text{const}$. The functions $f_{0,1}(x,t)$ and $U(x,t)$ are arbitrary at this step, so that formally one can analyze Eq. (3) from various viewpoints; however, even partial solution to Eq. (3) with an arbitrary function $U(x,t)$ is unknown [16]. This is why Eq. (3) can be considered from two different sides.

A. Approach from $U(x)$

At the first step, one can resolve Eq. (3) relative to the functions $U(x)$ and $U^*(x)$:

$$\frac{\partial U}{\partial x}+\left[2i\eta-\frac{\partial^2 f_0}{\partial x^2}\left(\frac{\partial f_0}{\partial x}\right)^{-1}\right]U-q^2 f_0\left(\frac{\partial f_0}{\partial x}\right)^{-1}U|U|^2=0, \tag{4a}$$

$$\frac{\partial U^*}{\partial x}+\left[-2i\eta-\frac{\partial^2 f_1}{\partial x^2}\left(\frac{\partial f_1}{\partial x}\right)^{-1}\right]U^*-q^2 f_1\left(\frac{\partial f_1}{\partial x}\right)^{-1}U^*|U|^2=0, \tag{4b}$$

where $q^2=q_0 q_1$. Algebraic manipulations with Eqs. (4) give a pair of Bernoulli equations for $|U|^2$ expressed in terms of the functions $f_{0,1}(x,t)$, which have general solutions:

$$\begin{aligned}|U|^2&=\left(\frac{\partial f_0}{\partial x}\right)\left(\frac{\partial f_0^*}{\partial x}\right)\times[C_0-q^2 f_0 f_0^*]^{-1}\\&=\left(\frac{\partial f_1}{\partial x}\right)\left(\frac{\partial f_1^*}{\partial x}\right)\times[C_1-q^2 f_1 f_1^*]^{-1}.\end{aligned} \tag{5}$$

Here, $C_{0,1}$ are the complex-valued integration constants. Now one can substitute $|U|^2$ into the last terms of Eqs. (4) and resolve them relative to $U(x)$ or $U^*(x)$, so that, for example,

$$\begin{aligned}U(x)=C_U&\left(\frac{\partial f_0}{\partial x}\right)\\&\times\exp\left\{-2i\eta x+q^2\int f_0\left(\frac{\partial f_0^*}{\partial x}\right)\times[C_0-q^2 f_0 f_0^*]^{-1}\mathrm{d}x\right\},\end{aligned} \tag{6}$$

where C_U is the complex-valued integration constant. This approach gives an opportunity to choose desirable complex-valued profiles of the slow acoustic wave $U(x)$ to grow weakly coupled acousto-optical states of the given shapes.

Let us consider two examples of not quite conventional profiles for acoustic components of the coupled states with some phase mismatches. One of these examples is the Gaussian profile $f_0(x)=B\exp(-bx^2)\exp(ip_0 x)$, where the constants B and b describe the amplitude and width, respectively, of this profile. With $C_0=B^2q^2[1+(p_0^2/b^2)]$ and $p_0=2\eta$, Eqs. (5) and (6) give us

$$|U|^2=\frac{4b^2(\eta^2+b^2x^2)}{q^2[(b^2+4\eta^2)\exp(2bx^2)-b^2]}, \tag{7a}$$

$$U(x) = 2BC_U(i\eta - bx) \times \exp\left\{-bx^2 + 2\int \frac{(bx + i\eta)\mathrm{d}x}{1 - \exp[2bx^2 \cdot \{1 - (4\eta^2/b^2)\}]}\right\}. \quad (7b)$$

The second example represents the Jacobi elliptic function

$$f_0 = Bcn(bx, m) \cdot \exp(ip_0 x), \quad (8)$$

where m is the elliptic modulus ($0 \le m \le 1$). With $C_0 = B^2q^2[1 + (p_0^2/b^2)]$ and $p_0 = 2\eta$, Eq. (5) gives

$$|U|^2 = \left(\frac{b^2}{q^2}\right)\frac{4\eta^2 cn^2(bx, m) + b^2 dn^2(bx, m)sn^2(bx, m)}{4\eta^2 + b^2 sn^2(bx, m)}. \quad (9)$$

Varying the elliptic modulus m, one can obtain either trigonometric or hyperbolic function realizations:

$$|U|^2 = \left(\frac{b^2}{q^2}\right)\cdot\frac{4\eta^2\cos^2(bx) + b^2\sin^2(bx)}{4\eta^2 + b^2\sin^2(bx)}, \qquad m = 0; \quad (10a)$$

$$|U|^2 = \left(\frac{b^2}{q^2}\right)\frac{\mathrm{sech}^2(bx)[4\eta^2 + b^2\tanh^2(bx)]}{4\eta^2 + b^2\tanh^2(bx)}, \qquad m = 1. \quad (10b)$$

When $p_0 = 2\eta = 0$, one yields

$$|U|^2 = \left(\frac{b^2}{q^2}\right) = \text{const}, \quad \text{with } m = 0; \quad (11a)$$

$$|U|^2 = \left(\frac{b^2}{q^2}\right)\cdot\mathrm{sech}^2(bx), \qquad \text{with } m = 1. \quad (11b)$$

In its turn, Eq. (6) gives $U(x)$ in all these cases. Thus in the general case, Eqs. (3), (8), and (10) with $p_0 = 2\eta$ serve as a good illustration to the approach presented. However, because the general solution to Eq. (3) is unknown [16], the effect of mismatches can be followed only in the particular cases.

B. Approach from $f_{0,1}(x)$

At the second step, we take the specific form of the function $U(x)$ with the stationary phase and put $U = U_0\exp(i\varphi)$, where U_0 is the real-valued amplitude, while the phase φ is a constant. As a result, Eq. (3) will be converted to

$$\frac{\partial^2 f_{0,1}}{\partial x^2} - \left[\pm 2i\eta + \left(\frac{1}{U_0}\right)\left(\frac{\partial U_0}{\partial x}\right)\right]\frac{\partial f_{0,1}}{\partial x} + q^2U_0^2 f_{0,1} = 0. \quad (12)$$

A similar selection of the function $U(x)$, which excludes the contribution of mismatches, looks more practical from the viewpoint of experimental realization and gives an opportunity to investigate the effect of mismatches on the light fields $f_{0,1}(x)$ and clarify their contributions in the efficiency of localization.

1. Hyperbolic-Secant Shape Acoustic Pulse

Let us take an analytic function U_0 with infinite support, namely, a hyperbolic-secant shape acoustic pulse of unknown amplitude H and the inversed duration σ, so that the boundary conditions (and localization conditions as well) have to be formulated for infinite distance. The phase parameter should be zero due to U_0 is the real-valued. Thus, with $U_0 = H\,\mathrm{sech}(\sigma x)$, Eq. (12) for the function $Y_0 \equiv f_0$, i.e., with upper sign in the squared brackets, can be rewritten as

$$\frac{\partial^2 Y_0}{\partial x^2} + [-2i\eta + \sigma\tanh(\sigma x)]\frac{\partial Y_0}{\partial x} + q^2H^2\,\mathrm{sech}^2(\sigma x)\cdot Y_0 = 0. \quad (13)$$

A project for the first exact solution (for the scattered light wave) to this equation can be taken as

$$y_0 = B\,\mathrm{sech}(Bx)\cdot\exp(ip_0 x), \quad (14)$$

where the amplitude and inversed duration B, and phase parameter p_0 are unknown. Substituting Eq. (14) into Eq. (13), one can find that Eq. (13) will be exactly satisfied if $p_0 = 2\eta$ and $\sigma = B = qH$. By this it means that the function f_0 includes the initially inserted phase mismatch η, while the amplitude of light pulses as well as their inversed durations are determined by the acoustic pulse amplitude H and properties of a material via the factor q. Thus Eq. (14) represents a partial solution y_0 to Eq. (13), and one can try to find the general solution to Eq. (13) [16] in the form

$$Y_0 = Z_1^{(0)}\sigma\,\mathrm{sech}(\sigma x)\cdot\exp(2i\eta x) + Z_2^{(0)}\cdot\frac{2i\eta + \sigma\tanh(\sigma x)}{\sigma(\sigma^2 + 4\eta^2)}, \quad (15)$$

where $Z_{1,2}^{(0)}$ are the integration constants. The function $Y_1 \equiv f_1$ has the form similar to Eq. (15), but with the opposite sign of η and the integration constants $Z_{1,2}^{(1)}$. Exploiting the conservation law $|Y_0|^2 + |Y_1|^2 = J_0^2$ with the boundary conditions $|Y_0|^2(x \to \pm\infty) = 0$ and $|Y_1|^2(x \to \pm\infty) = J_0^2$, one can obtain

$$|Y_0|^2(x) = \frac{J_0^2\sigma^2}{\sigma^2 + 4\eta^2}\mathrm{sech}^2(\sigma x), \quad (16a)$$

$$|Y_1|^2(x) = J_0^2\cdot\frac{4\eta^2 + \sigma^2\tanh^2(Ax)}{\sigma^2 + 4\eta^2}. \quad (16b)$$

Additionally, one can say that the initially chosen function $U_0 = q^{-1}\sigma\,\mathrm{sech}(\sigma x)$ exhibits the simplest example of localization, i.e., a one-pulse weakly coupled state, with infinite support for the amplitude U_0.

2. Rectangular Acoustic Pulse

Here, we choose the amplitude U_0 in the form of a generalized function with compact support. Namely, a solitary rectangular pulse is taken, so that the available distance of localization is physically restricted by this pulse width. Now both the boundary conditions and the localization conditions have to be formulated for a limited distance due to a compact support of the amplitude U_0. The real-valued amplitude function can be expressed as $U_0 = H\,\mathrm{rect}(x/L_0)$, where $\mathrm{rect}(\xi) = 1$ only when $|\xi| \le 1/2$, and $\mathrm{rect}(\xi) = 0$ when $|\xi| > 1/2$, so that the compact support is restricted by the interval $[-L_0/2, L_0/2]$. As a result, Eq. (12) can be rewritten as

$$\frac{\partial^2 f_{0,1}}{\partial x^2} \mp 2i\eta \frac{\partial f_{0,1}}{\partial x} + \sigma^2 f_{0,1} = 0 \tag{17}$$

only in an area inside this acoustic pulse, i.e., inside the chosen localization distance where $\sigma^2 = q^2 H^2$. For the area lying outside of that acoustic pulse, the acousto-optical interaction is absent, and the localization conditions have to be formulated only within that area. The exact general solution to Eq. (17) is given by

$$f_{0,1} = P_{0,1} \exp\left[ix\left(\pm\eta - \sqrt{\sigma^2+\eta^2}\right)\right] + Q_{0,1} \exp\left[ix\left(\pm\eta + \sqrt{\sigma^2+\eta^2}\right)\right], \tag{18}$$

where $P_{0,1}$ and $Q_{0,1}$ are the complex-valued integration constants. The intensities $|F_{0,1}|^2$ of light waves inside the acoustic pulse can be expressed as $|F_{0,1}|^2 \equiv |f_{0,1}|^2$ in this case. Thus one can require $|F_0|^2(x=0) = J_0^2$, $|F_1|^2(x=0) = 0$ and find

$$|F_1|^2 = \frac{J_0^2\sigma^2}{\sigma^2+\eta^2} \cdot \sin^2\left(x\sqrt{\sigma^2+\eta^2}\right), \tag{19a}$$

$$|F_0|^2 = J_0^2\left[\frac{\eta^2}{\sigma^2+\eta^2} + \frac{\sigma^2}{\sigma^2+\eta^2} \cdot \cos^2\left(x\sqrt{\sigma^2+\eta^2}\right)\right]. \tag{19b}$$

Due to Eq. (19) being valid only inside the finite interval of existing the acoustic pulse, one may discuss localization only relative to a compact support for the amplitude function $U_0 = q^{-1}\sigma\,\mathrm{rect}(x/L_0)$, which restricts an area of realizing the acousto-optical interaction. Physically, the solutions, described by Eqs. (16) and (19), involve contributions of two types. For the incident light, one can identify first the contribution of some backgrounds, which are independent on the coordinate x, and then some oscillating portions of the solutions, describing localization of the incident light. These oscillating portions are imposed on the corresponding backgrounds, whereby just the existence of joint angular-frequency mismatch η as well as its magnitude determines the value of those backgrounds.

3. SUPPORT OF SOLITARY PROFILES INHERENT IN WEAKLY COUPLED STATES

The Jacobi elliptic functions are doubly periodic functions whose primitive periods ratio is not real [17]. In particular, the periodicity is characterized by $4KN + 2iK'M$ for $sn(z,m)$, $4KN + 2(K+iK')M$ for $cn(z,m)$, and $2KN + 4iK'M$ for $dn(z,m)$. Here, $K(m)$ is complete elliptic integral of the first kind, and $K'(m) = K(m')$ with $m' = 1-m$, while $N, M = 0, \pm1, \pm2, \ldots$ [18]. These functions are real-valued for real argument z and real modulus m when $0 \le m \le 1$. Initially, we restrict ourselves by a pair of the factors $(N=1, M=0)$ and consider the functions $dn(z,m)$ (see Fig. 1), $sn^2(z,m)$, and $cn^2(z,m)$ (see Fig. 2) within their first primitive period determined by $2K(m)$. Mathematically trivial variation of their periods from π to infinity as m grows from zero to unity acquires specific physical meaning. The plots in Figs. 1 and 2 demonstrate that when $N=1$ and $M=0$, the interval $[-K(m), K(m)]$ can be considered as the complete interval of existing the support for cnoidal solitary profiles, and this interval of existing the support is a function of the modulus m.

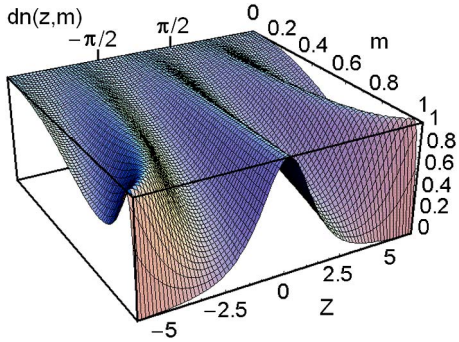

Fig. 1. Acoustic component. With growing m, initially a rectangular pulse of the finite width π, creating a compact support, is converted into a hyperbolic secant pulse giving infinite support for optical components of the coupled state.

In particular, Fig. 1 demonstrates the evolution of the cnoidal acoustic pulse profile $|U(z)| = dn(z,m)$, i.e., the conversion of a rectangular distribution $dn(z,0)$ at the compact support $[-K(0) = -\pi/2, K(0) = \pi/2]$ to a hyperbolic profile $dn(z,1) = \mathrm{sech}(z)$ with infinite support, because of $K(1) \to \infty$. The same behavior demonstrates the cnoidal light intensity profiles $sn^2(z,m)$ and $cn^2(z,m)$ (see Fig. 2) evolving from trigonometric profiles $|f_1|^2(z) = \sin^2(z)$, $|f_2|^2(z) = \cos^2(z)$ with $m=0$ and compact support $z \in [-\pi/2, \pi/2]$ to hyperbolic profiles $|f_1|^2(z) = \tanh^2(z)$, $|f_2|^2(z) = \mathrm{sech}^2(z)$ with $m=1$ and infinite support $z \in [-\infty, \infty]$. In other words, this explanation represents an alternative view on determining the conditions of localization. Namely, traditionally exploited infinite distance of localization corresponding to infinite support for solitary profiles such as Gaussian or hyperbolic ones can be considered as a limit of more general view including the cases of compact supports; for example, for cnoidal profiles with $m < 1$ and $K(m) < \infty$. The compact support can be naturally motivated physically here via choosing the acoustic pulse width restricted by the value $2K(m)$, since acousto-optical interaction is absent outside this pulse. To obtain a qualitative insight into evolving the cnoidal profiles with a mismatch in an area of relatively small moduli m (i.e., for quasi-trigonometric profiles), one can exploit the approximate expressions [18]

$$sn(z,m) \approx \sin(z) - \frac{m}{4}[z - \sin(z)\cos(z)]\cos(z), \tag{20a}$$

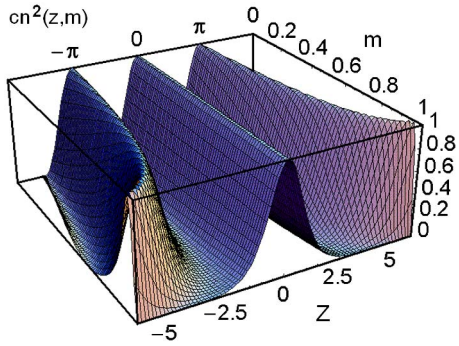

Fig. 2. Optical component. Initially trigonometric profile with compact support π is transformed into a hyperbolic profile with infinite support as the modulus m grows from zero to unity.

$$cn(z,m) \approx \cos(z) - \frac{m}{4}[z - \sin(z)\cos(z)]\sin(z) \qquad (20b)$$

with $z = x\sqrt{\sigma^2 + \eta^2}$ and under condition $m^2 \ll m$, i.e., practically with $0 \le m \le 0.4$.

The discussed possibilities were related to single-pulse profiles due to taken above restriction by the case ($N = 1$, $M = 0$). However, keeping $M = 0$, one can consider the cases with $N > 1$. The performed analysis demonstrates that cnoidal profiles allow existing various multipulse, i.e., N-pulse profiles, depending on a number of the periods $2K(m)$ selected as the compact support. Consequently, one can consider a condition of localization, which is perfectly characterized by compactness of support, for the scattered light intensity within the distance L_0 of acousto-optical interaction and find that $L_0\sqrt{\sigma^2 + \eta^2} = 2K(m)N$, so that the localization distance can be taken; for instance, to be $L_0 = L$. The scattered light intensity will be nonzero only in the spatial interval occupied the nonoptical wave; therefore the envelope of the scattered wave will be localized. Namely, its distribution inside the acoustic pulse will have N partial peaks in its envelope, while the optical pump intensity will have N holes. When all these phenomena occur, one may say that an N-pulse dissipative coupled state is shaped within a three-wave collinear light scattering. The number N of bright or dark pulses in optical components of any dissipative coupled state is connected with the frequency mismatch η as $\eta^2 = 4K^2(m)N^2L_0^{-2} - \sigma^2$.

To consider the dynamics in the lossy case, one has to introduce an additional coordinate parameter $\xi \sim Vt$ that determines current positions of weakly coupled states in a process of its propagation through a crystal. In so doing, one can follow evolving various cases of the light intensity distributions $|a_0|^2(x)$ and $|a_1|^2(x)$ in the weakly coupled acousto-optical states. For the initially chosen profile $U_0 = q^{-1}\sigma\mathrm{sech}[\sigma(x - \xi)]$, describing hyperbolic secant shape lossless acoustic pulse, one can write

$$|a_0|^2(x,\xi) = \frac{J_0^2\sigma^2}{\sigma^2 + 4\eta^2}\mathrm{sech}^2[\sigma(x - \xi)]\exp(-2\alpha x), \qquad (21a)$$

$$|a_1|^2(x,\xi) = J_0^2\exp(-2\alpha x)\frac{4\eta^2 + \sigma^2\tanh^2[\sigma(x - \xi)]}{\sigma^2 + 4\eta^2}. \qquad (21b)$$

For the lossless rectangular acoustic pulse of the same amplitude $q^{-1}\sigma$, one can write

$$|a_0|^2(x,\xi) = J_0^2\left[\frac{\eta^2}{\sigma^2 + \eta^2} + \frac{\sigma^2}{\sigma^2 + \eta^2}\cdot\cos^2\left[(x - \xi)\sqrt{\sigma^2 + \eta^2}\right]\right] \times \exp(-2\alpha x), \qquad (22a)$$

$$|a_1|^2(x,\xi) = \frac{J_0^2\sigma^2}{\sigma^2 + \eta^2}\sin^2\left[(x - \xi)\sqrt{\sigma^2 + \eta^2}\right]\exp(-2\alpha x). \qquad (22b)$$

Exploiting Eqs. (21) and (22), one can follow the corresponding dynamics for these pulses with, for example, $L = 2$, $J_0 = q = 1$, $\alpha = 0.1$, and $\sigma = 10$ (see Fig. 3).

4. CHARACTERIZING THE SOLITARY PROFILES OF WEAKLY COUPLED STATES

Now let us determine the localization distance (or, what is the same, the pulse width) L_0 as the function of the mismatch η

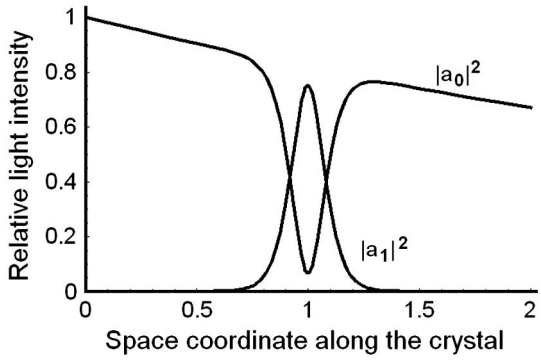

(a) $\xi = 1.0$

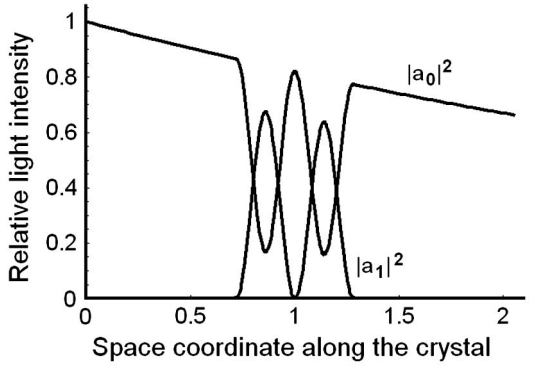

(b) $\xi = 0.72$

Fig. 3. Evolution of the optical components $|a_0|^2$ and $|a_1|^2$ in the weakly coupled acousto-optical states. (a) Hyperbolic profiles with $\eta = 1.5$, infinite support. (b) Trigonometric profiles with $\eta = 5$, $N = 2$, the compact support $L_0 \approx 0.562$.

with $\sigma = \{0.5, 1.0, 2.0, 3.0\}$ as a parameter. For a hyperbolic profile, "full width" of the corresponding pulse with infinite support will be conditionally taken at the intensity level 0.01, so that one has

$$\text{Trigonometric profile:} L_0 = \pi N/\sqrt{\sigma^2 + \eta^2}, \qquad (23a)$$

$$\text{Hyperbolic profile:} L_0 = 2\sigma^{-1}\mathrm{arcsech}\{0.1\cdot[1 + (4\eta^2/\sigma^2)]^{1/2}\}. \qquad (23b)$$

One can see from Fig. 4 that growing σ leads to decreasing the expected localization distance L_0, i.e., reducing the localization distance even with $\eta = 0$. Then the appearance of the mismatch as well as its gain shorts further the localization distance. Then one can characterize the combined dependences for the needed mismatch η, which provides shaping the weakly coupled states of a given localization distance L_0 (at the intensity level 0.01 for hyperbolic secant profile) and relative efficiency of localization Ef as the functions of the parameter σ.

$$\text{Trigonometric profile:} \eta = \sqrt{\pi^2N^2L_0^{-2} - \sigma^2}, \quad Ef = \sigma^2(\sigma^2 + \eta^2)^{-1}; \qquad (24a)$$

$$\text{Hyperbolic profile:} \eta = (\sigma/2)\sqrt{100\,\mathrm{sech}^2(\sigma L_0/2) - 1}, \quad Ef = \sigma^2(\sigma^2 + 4\eta^2)^{-1}. \qquad (24b)$$

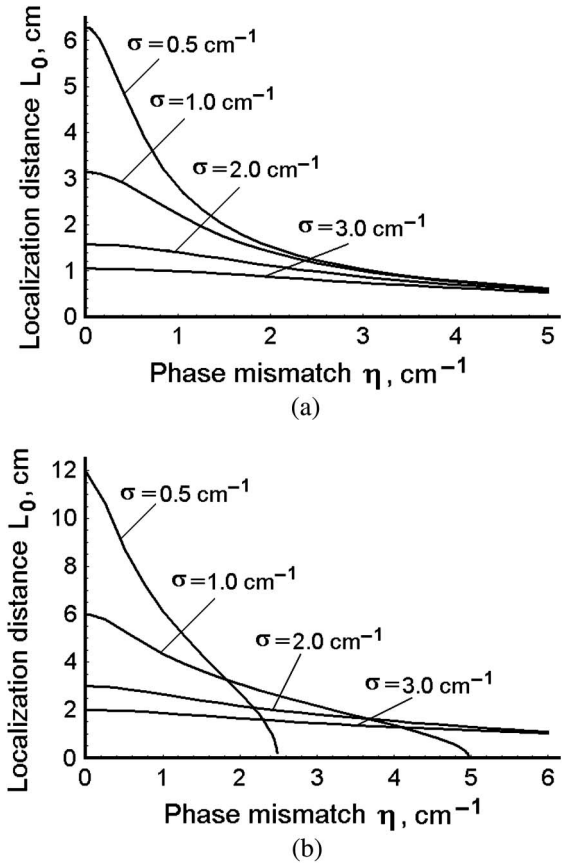

Fig. 4. Localization distance L_0 versus the mismatch η with σ as a parameter: (a) for trigonometric profile with $N = 1$ and (b) for hyperbolic secant profile.

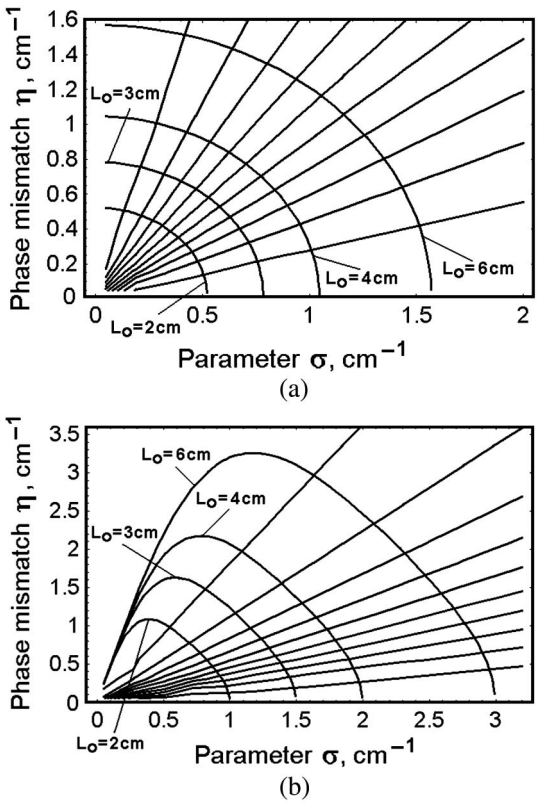

Fig. 5. Localization distance L_0 and relative efficiency of localization Ef on the plane $\{\sigma, \eta\}$. (a) Trigonometric profile with $N = 1$ and (b) for hyperbolic secant profile.

The corresponding plots are depicted in Fig. 5. The relative efficiency of localization does not depend on optical losses because this parameter takes into account only interrelation between two optical components attenuating in accordance with the same law. As a result, there are fans of direct rays representing the same efficiency for each individual ray on the plane $\{\sigma, \eta\}$. These rays are starting from the coordinate origin in such a way that a smaller tangent of a ray corresponds to a higher efficiency of localization, so that the horizontal ray gives unit efficiency. While larger tangents reflect lower efficiency, and the vertical line gives zero one.

One can see that growing σ leads to decreasing the mismatch η with the chosen distance L_0. The efficiency of localization grows in accordance with σ as faster as the localization distance L_0 is longer.

To illustrate the contribution of linear optical losses let us restrict ourselves by the case of availability of Eq. (22). Two examples of intensity distributions for the optical component $|a_1|^2$ inherent in three-wave weakly coupled state at the fixed $J_0 = 1$ and $\xi = 0$ versus both the dimensionless ratio (η/σ) and the dimensionless product (αx) characterizing optical losses are shown in Fig. 6. One can see from these 3D plots that doubling the ratio σ/α via growing acoustic power density or decreasing linear optical losses at $\eta/\sigma = 0$ leads to the transition from a one-pulse state to a two-pulse one. Thus the practical aspects of realizing and observing three-wave acousto-optical coupled states in media with optical losses are another than in the case of nonoptical losses [15]. Linear optical losses affect both the conditions of shaping weakly coupled states as well as the process of their observation (see Section 7). This is why, to identify the dissipative coupled states under consideration, one has to estimate a set of the simulations reflecting experimental conditions. These conditions include the chosen lengths of interaction and level of optical losses, which both can be varied only by changing the crystalline cell.

5. ESTIMATIONS FOR ACOUSTO-OPTICAL REALIZATION OF THE WEAKLY COUPLED STATES IN COLLINEAR α-QUARTZ CELL WITH LINEAR OPTICAL LOSSES

The α-quartz (i.e., α-SiO_2) had been chosen as an appropriate acousto-optical material for two reasons. First, rather developed technology, based on the controlled x-ray irradiation, exists for manufacturing α-quartz samples with a predicted optical transmission. Second, it is well known [19] that collinear acousto-optical cell can be successfully realized with this crystalline material. Using the propagation of pure longitudinal elastic mode ($V_L = 5.72 \cdot 10^5$ cm/s) along the [100] axis. The Bragg regime of light scattering requires $Q = 2\pi\lambda L f^2/(nV^2) \geq 4\pi$ for the Klein–Cook parameter [20]. Taking $\lambda = 633$ nm, $n = 1.55$, and $L = 6.0$ cm, one yields $Q \approx 12.5$ for the acoustic frequencies $f \geq 46$ MHz wherein the Bragg regime is expected. Then one can find [21] the effective photoelastic constant $p_{ef} = p_{41}$ and the figure of acousto-optical merit $M_2 = 0.15 \cdot 10^{-18}$ s^3/g for anomalous collinear interaction within similar geometry.

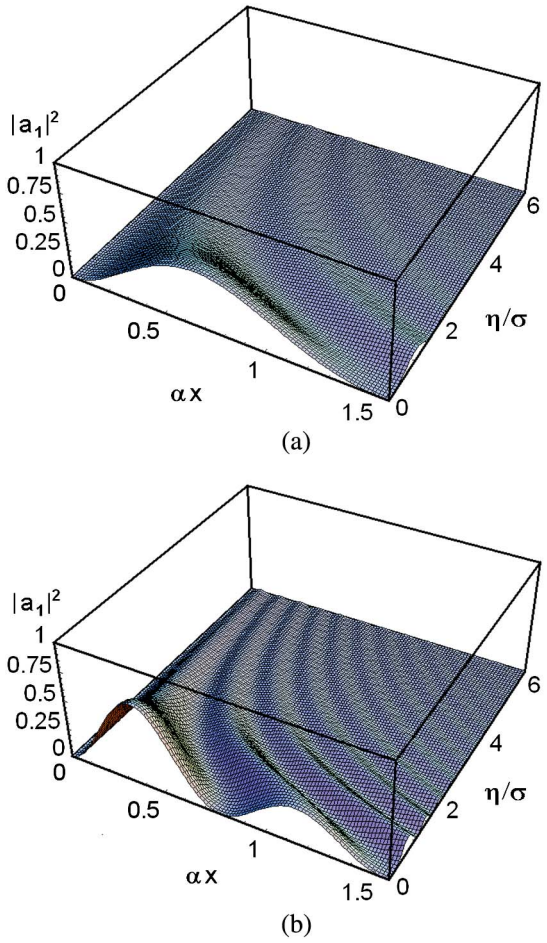

Fig. 6. Light intensity $|a_1|^2$ of three-wave weakly coupled state at $J_0 = 1$ and $\xi = 0$ versus the ratio (η/σ) and the product (αx): (a) is for $\sigma/\alpha = 2.0$ and (b) is for $\sigma/\alpha = 4.0$.

Let us estimate a contribution of the acoustic losses in an AOC with $L = 6$ cm. The characteristic acoustic frequency f_0 inherent in collinear interaction at $\lambda = 633$ nm in this α-quartz cell is $f_0 = \Delta n V_L/\lambda \approx 81.327$ MHz, where $\Delta n = 0.009$ is the difference between main refractive indices for ordinary and extraordinary light modes. The total level γ of losses along the collinear cell's aperture $L = 6$ cm is equal to $\gamma = \Gamma L f_0^2 \cong 0.12$ dB, where $\Gamma = 3.0$ dB/(cm · GHz^2) is the factor of losses for the longitudinal acoustic wave [21]. The obtained γ is so small that this AOC can be considered as acoustically lossless.

Now one has to find acoustic power needed for observing at least the first period ($N = 1$) of localizing the scattered light field. The estimations show that with $\eta = 0$ the needed acoustic power density $P = 2\lambda^2\sigma^2/(\pi^2 M_2)$ even for $N = 1$ is too high for experimental realization, because performances inherent in the piezoelectric transducer with the area 4 mm^2 do not allow significant excess of $P \cong 1$ W/mm^2, which is associated with $\sigma \le 0.5$ cm^{-1} for this AOC. For trigonometric profiles with $N = 1$ and $\eta = 0$, one has to provide $\sigma = \pi/L_0$ or even $\sigma = \pi N/L_0$ when $N \ge 1$. These equalities are based on the periodicity equal to πN at a zero light intensity level, which is peculiar for the exploited trigonometric functions. For hyperbolic functions, one meets another situation. With $\eta = 0$, one has to provide $\sigma \approx 6/L_0$ at the above-chosen almost-zero light-intensity level 0.01. This is why one has to consider the possibilities related to $\eta \neq 0$ and to formulate modified practical estimations.

Table 1. Estimations Using α-Quartz Crystal with $L_0 = 6$ cm, $\sigma = 0.43$ cm^{-1}, and Obtaining the Needed Acoustic Power Density $P = 1.0$ W/mm^2 for the Three Cases

Optical Profile	η(cm^{-1})	Δf(kHz)	N	Relative Efficiency Ef.
Hyperbolic	0.4	72.829	1	0.038
Trigonometric	0.3	54.622	1	0.7
Trigonometric	0.9	163.866	2	0.2

It should be noted that, broadly speaking, one can expect losses of acoustic energy via a mechanism of the second-harmonic generation for the longitudinal acoustic mode passing along the [100] axis in α-SiO_2. Nevertheless, using the approach developed in [22], one can estimate that similar losses are negligibly small due to rather low efficiency of such a conversion at $P \cong 1$ W/mm^2 in α-quartz crystal.

As determined initially, $\Delta f = \eta V/\pi$, so that for α-SiO_2 one can write $\Delta f(\text{kHz}) = \eta V_L/\pi \approx 182 \cdot \eta(\text{cm}^{-1})$. By this, it means that effect of localizing the scattered light with hyperbolic and trigonometric profiles as well as shaping the hyperbolic and trigonometric shape dissipative coupled states with the phase mismatch can be identified and observed. The theoretical results are listed in Table 1. Finally, one can estimate that with $\alpha = 0.1$ cm^{-1} and $L = 6$ cm, optical losses give the factor $\exp(-2\alpha L) \approx 0.3012$, which cannot be considered as insignificant.

6. SCHEME FOR EXPERIMENTS WITH THE α-QUARTZ COLLINEAR CELL

To realize experimentally the process of collinear interaction, we have used the scheme shown in Fig. 7. It consists of a continuous-wave laser, a α-SiO_2-crystalline AOC with a pair of the Glan–Taylor crystalline polarizers (with the extinction ratio 10^5 each), a wide-aperture silicon photo-detector, and a set of electronic equipment for both generating and registering the corresponding electric very-high-frequency (VHF) radio-wave signals. Initially, the needed shape of the modulating envelope is provided by the amplitude modulator represented by the arbitrary waveform generator (AWG2021, Sony). Then a tunable radio-wave signal is applied to the electronic input port of the collinear AOC cell through a wideband VHF amplifier HD18858 (10–1000 MHz, 8 W) (see Fig. 7) and to the input of an oscilloscope (computer) as the etalon signal. This electronic signal excites the piezoelectric transducer, which

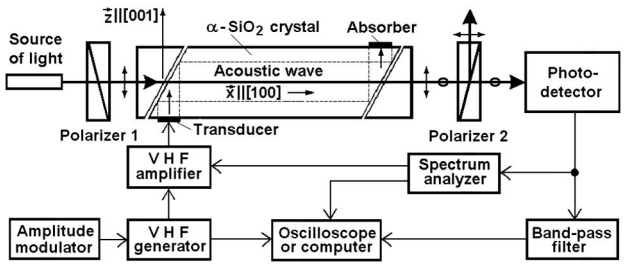

Fig. 7. Schematic arrangement of the experimental setup.

generates the pure longitudinal acoustic wave with the corresponding carrier frequency. Together with this, the variable analogue signal from the VHF generator synchronizes the oscilloscope and determines the horizontal scale of a sweep. At the same time, the detected light signal goes through the bandpass filter and shapes the digitized oscilloscope trace on the display of an oscilloscope or computer.

A two-mode co-propagating collinear AOC had an active acousto-optical aperture of about $L = 6$ cm along the [100] axis. The piezoelectric transducer was made of a thin ($Y + 36°$) cut lithium niobate crystalline plate, so that it excited the purely longitudinal acoustic wave with conversion losses of about 2 dB. The acoustic-power density slightly exceeding 1.0 W/mm^2 was provided at its resonant frequency close to 81.3 MHz inside the collinear AOC after reflection by the left declined facet. In its turn, the right declined facet of the α-quartz crystal directed the residual acoustic power to the absorber. The continuous-wave light beam (from CrystaLaser solid-state laser; the output optical power $\geq$50 mW; $\lambda = 633$ nm; transverse mode TEM$_{00}$; single longitudinal mode, providing narrow enough optical spectral line) had been used as an optical pump during the experiments with the traveling-wave regime of interaction between the pump and the acoustic wave of finite amplitude. The amplitude factor α of the linear optical losses was about 0.1 cm^{-1} (i.e., about 0.87 dB/cm) inherent in the x-ray slightly irradiated α-quartz crystal exploited at the chosen optical wavelength. The level of irradiation was enough to increase markedly linear optical losses but is too low to change measurably the other acoustic and acousto-optical properties of α-quartz crystal [21]. This is why a pair of not irradiated quartz prisms had been used to exclude their effect on the subject of studies. The outside facets of these prisms had an antireflection coating. At least two regimes of operation were used to estimate the frequency dependencies at stepwise variations of the applied acoustic power. They both include exploitation of the sweep-generator from spectrum analyzer and provide operating with the bandpass filter (bandwidth ~5 kHz) and oscilloscope as well as with the spectrum analyzer (bandwidth $\leq$10 Hz), in particular, for calibrations and accurate measurements of frequency. After the interaction with the acoustic wave, the scattered light beam passed to the photo-detector through the second polarizer giving us an opportunity to extract a well-cleaned portion of the output optical signal. Slowly varying electronic responses from the silicon photo-detector were exploited for filtering and shaping the digitized oscilloscope traces.

7. BRIEF DISCUSSION

The physical possibility of shaping optical components inherent in three-wave weakly coupled acousto-optical states has been followed within our experiments. The measurements have been performed with the controlled phase mismatches under action of the corresponding acoustic pulses of finite amplitude. During all experiments carried out, the acoustic power density and the wavelength of a continuous-wave optical beam were fixed at the level of about $P \approx 1$ W/mm^2 (i.e., at $\sigma \approx 0.43$ cm^{-1}) and $\lambda \approx 633$ nm.

As explained above, two limiting cases of the solitary cnoidal waves, namely, trigonometric and hyperbolic profiles, have been chosen for experimental verifications of the developed theory.

The phenomenon of shaping and localizing the optical components of dissipative weakly coupled acousto-optical states has been sequentially followed during our experiments for the collinear geometry of three-wave interaction. The scattered light wave components inherent in collinear dissipative weakly coupled states have been observed in the irradiated α-SiO_2 collinear AOC providing the length of acousto-optical interaction $L = 6$ cm. In the frames of these measurements, the chosen frequencies were about $f_H \approx 81.426$ MHz for hyperbolic shape pulses and $f_{(1)} \approx 81.408$ MHz and $f_{(2)} \approx 81.517$ MHz for trigonometric shape pulses with $N = 1, 2$, respectively. The main lobe of efficiency for collinear acousto-optical interaction was estimated in width as $\delta f \approx 96.113$ kHz for the cell exploited. In these cases, the acoustic power was varied from zero to $P(\Delta f_{(1)}) \approx P(\Delta f_{(2)}) \approx 4$ W.

Due to the fact that linear optical losses affect significantly the processes of both evolving and detecting the optical components of weakly coupled acousto-optical states, one could expect that only a portion of linearly polarized light intensity, injected initially into material of the AOC, will be registered by the output photo-detector (Fig. 7). The direct measurements have confirmed that total residual light intensity at the AOC's output prism facet is close to 30% of the light beam detected at the input prism facet of the AOC (both these facets of prisms had an antireflection coating) taking into account the corrections related to reflections from intermediate optical surfaces of this cell. After that, all the oscilloscope traces had been normalized by the obtained level of light intensity. Undoubtedly, the accuracy of such an approach to normalization can be a subject for some insignificant refining, but nevertheless we

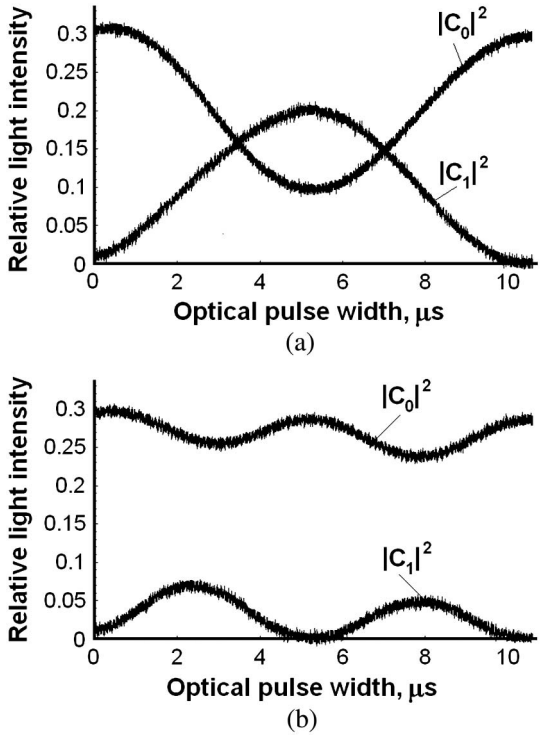

Fig. 8. Digitized oscilloscope traces for the transmitted $|C_0|^2$ (upper traces) and scattered $|C_1|^2$ (lower ones) light intensities observed at the output of the above-described α-quartz collinear AOC under action of a rectangular acoustic pulse of finite amplitude and time width about 10.5 μs: (a) $N = 1$, $f_{(1)} \approx 81.408$ MHz and (b) $N = 2$, $f_{(2)} \approx 81.517$ MHz.

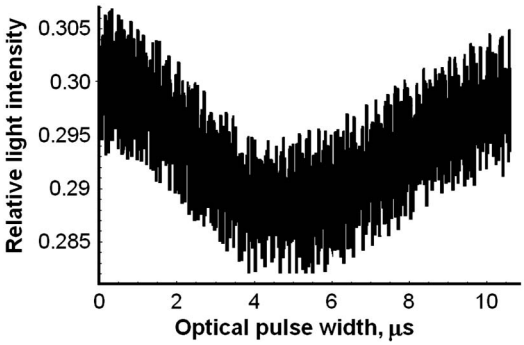

(a) $|C_0|^2$.

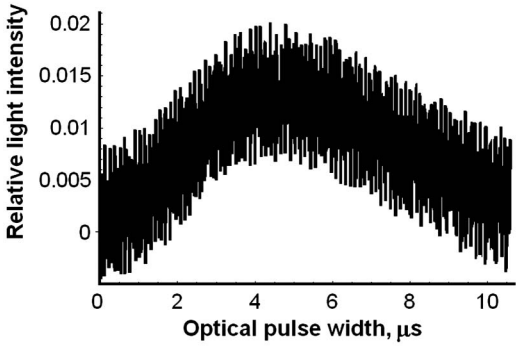

(b) $|C_1|^2$.

Fig. 9. (a) Digitized oscilloscope traces for the transmitted light $|C_0|^2$ and (b) scattered light $|C_1|^2$ intensities observed at the output of the above-described α-quartz collinear AOC at the acoustic frequency $f_H = 81.426$ MHz under action of a hyperbolic secant acoustic pulse of finite amplitude and time width about 10.5 μs at the acoustic intensity level 1%.

consider the estimated (in such a way) correlations between the detected intensities of optical components as sufficiently adequate to real ratios. A few examples of the corresponding digitized oscilloscope traces peculiar to the desired optical components are shown in Figs. 8 and 9.

Excluding the efficiency of localization, which requires much higher acoustic-power density, the experimentally obtained oscilloscope traces can be qualitatively compared with the above-depicted theoretical curves for the optical components of the weakly coupled acousto-optical states shown in Fig. 3. For trigonometric profiles with $N = 2$, one can see direct correlations between plots in Figs. 3(b) and 7(b). Namely, they both exhibit two oscillations in the falling down transmitted and scattered light components within the corresponding compact supports determined by the acoustic pulse width. For hyperbolic profiles in their turn, one can find the correspondence between theoretical plots in Fig. 3(a) and traces in Fig. 8 reflecting the appearance of minimum and maximum in distributions of the transmitted and scattered optical components, respectively, within the registered portion of infinite support.

8. CONCLUDING REMARKS

The most important result of these measurements consists in the fact that the phenomenon of originating a set of three-wave weakly coupled acousto-optical states with the phase mismatches is experimentally confirmed and the expected optical components of these solitary waves have been revealed and detected. Levels of light intensities achieved on each of the obtained oscilloscope traces represent balances between the above-mentioned acoustic power density about $P \approx 1$ W/mm^2, which was close to the limit of electromechanical durability for the piezoelectric transducer exploited and the effect of the exploited phase mismatches. Then one can note critically important contributions of these phase mismatches, which made it possible to decrease essentially the applied acoustic power density associated with acoustic pulses of finite amplitude and prescribed profiles specifically in the case of hyperbolic profiles.

The observed oscilloscope traces with hyperbolic profiles have been detected at the signal-to-noise ratio that exceeds unity only slightly, i.e., it lies rather close to a border of practically reliable identification. Thus we have revealed and studied a specific regime for appearing and evolving three-wave dissipative solitary pulses. Namely, the three-wave weakly coupled states that occur due to collinear Bragg light scattering by a relatively slow acoustic wave of finite amplitude in a two-mode medium with square-law nonlinearity and linear optical losses have been investigated. A novel quasi-stationary analytic description of similar weakly coupled states with the phase mismatches has been developed. The proposed approach allows initiating analytic description of the mismatched weakly coupled states either from the acoustic wave of finite amplitude or from one of the optical components. The availability of compact and infinite support has been considered in detail using the cnoidal pulse profiles as an example. In connection with this, two limiting cases for cnoidal profiles have been characterized and estimated.

The arranged experimental setup made it possible to observe optical components inherent in the mismatched weakly coupled states via acousto-optical experiments. For this purpose, the specially created collinear AOC based on the x-ray irradiated α-quartz crystal, exhibiting the given optical losses, had been exploited. One can note rather good correspondence of the obtained numerical estimations with practically observed magnitudes of the frequency detuning, acoustic power density, and efficiency of localization within the proof-of-principle experiments carried out.

ACKNOWLEDGMENTS

This work has been financially supported by the CONACyT, Mexico, within the project no. 61237 (initially) and the INAOE Opto-Electronic Project.

REFERENCES

1. K. Dodd, J. C. Eilbeck, J. D. Gibbon, and H. Morris, *Solitons and Nonlinear Wave Equations* (Academic, 1984).
2. A. P. Sukhorukov, *Nonlinear Wave Processes* (Nauka, 1988).
3. Yu. S. Kivshar and G. P. Agrawal, *Optical Solitons: From Fibers to Photonic Crystals* (Academic, 2003).
4. I. G. Mikhailov and V. A. Shutilov, "Diffraction of light on the ultra sound waves of large amplitude," Akusticheskij Zhurnal **4**, 174–183 (1958), in Russian.
5. M. A. Breazcale and E. A. Hiedemann, "Diffraction patterns produced by finite amplitude waves," J. Acoust. Soc. Am. **33**, 700 (1961).
6. R. Torguet, C. Carles, E. Bridoux, and M. Moriamez, "Diffraction of light by finite amplitude acoustic waves in nonlinear crystals," in *Ultrasonics Symposium* (1972), pp. 147–150.
7. T. H. Neighbors and W. G. Mayer, "Asymmetric light diffraction by pulsed ultrasonic waves," J. Acoust. Soc Am. **74**, 146–152 (1983).

8. K. Van Den Abeele and O. Leroy, "Light diffraction by ultrasonic pulses: analytical and numerical solutions of the extended Raman–Nath equations," J. Acoust. Soc. Am. **88**, 2298–2315 (1990).
9. F. W. Windels, V. I. Pustovoit, and O. Leroy, "Collinear acousto-optic interaction using two nearby sound frequencies," Ultrasonics **38**, 586–589 (2000).
10. V. N. Parygin and A. V. Vershoubskiy, "Collinear diffraction of Gaussian optical beams by an acoustic pulse," Pure Appl. Opt. **7**, 733–746 (1998).
11. L. Adler, W. T. Yost, and J. H. Cantrell, "Subharmonics, chaos, and beyond," in *International Congress on Ultrasonics: Gdańsk 2011*, *AIP Conference Proceedings* (2012), Vol. **1433**, pp. 527–530.
12. A. S. Shcherbakov and A. Aguirre Lopez, "Shaping the optical components of solitary three-wave weakly coupled states in a two-mode waveguide," Opt. Express, **11**, 1643–1649 (2003).
13. A. S. Shcherbakov, S. E. Balderas Mata, Je. Maximov, and A. Aguirre Lopez, "The existence of five-wave non-collinear acousto-optical weakly coupled states," J. Opt. A **10**, 085106 (2008).
14. N. Akhmediev and A. Ankiewicz, *Dissipative Solitons* (Springer, 2005).
15. A. S. Shcherbakov, Je. Maximov, and S. E. Balderas Mata, "Shaping the dissipative collinear three-wave coupled states in a two-mode medium with a square-law nonlinearity and linear non-optical losses," J. Opt. A **10**, 025001 (2008).
16. A. D. Polyanin and V. F. Zaistev, *Handbook of Exact Solutions for Ordinary Differential Equations*, 2nd ed. (CRC, 2003).
17. E. H. Neville, *Elliptic Functions: A Primer* (Pergamon, 1971).
18. M. Abramowitz and I. A. Stegun, *Handbook of Mathematical Functions: With Formulas*, *Graphs*, *and Mathematical Tables* (Dover, 1964).
19. R. W. Dixon, "Acoustic diffraction of light in anisotropic media," IEEE J. Quantum Electron. **QE-3**, 85–93 (1967).
20. W. R. Klein and B. D. Cook, "Unified approach to ultrasonic light diffraction," IEEE Trans. Sonics Ultrason **14**, 123–134 (1967).
21. A. A. Blistanov, V. S. Bondarenko, N. V. Perelomova, N. S. Strizhevskaya, and V. V. Chkalova, in *Acoustic Crystals*, M. P. Shaskolskaya, ed. (Nauka, 1982).
22. A. S. Shcherbakov, D. Sánchez Lucero, A. Luna Castellanos, and O. I. Belokurova, "Direct multi-channel optical spectrum analysis of radio-wave signals using collinear wave heterodyning in single acousto-optical cell," J. Opt. **12**, 045203 (2010).